

Sensitive Colorimetric and Fluorimetric Probe for the Detection of Sodium valproate using Glutathione Capped Silver Nanoclusters

Asma Laghari and Muhammad Yar Khuhawar,

Dr. M.A. Kazi Institute of Chemistry, University of Sindh, Jamshoro, Sindh, Pakistan.

laghariasma88@gmail.com, mykhuhawar@usindh.edu.pk*

(Received on 6th March 2024, accepted in revised form 29th July 2024)

Summary: Silver nanoclusters were synthesized and passivated by glutathione (GSH) ligand, with high aqueous stable powerful red fluorescence and UV-Vis light yellow colour. A novel colorimetric and fluorimetric assays have been presented for the detection of sodium valproate using glutathione capped silver nanoclusters, (GSH-Ag NCs) as a colorimetric and fluorimetric sensor. The size of the AgNCs-GSH was found to be ~10 nm on DLS. The fluorimetric detection of GSH-AgNCs with sodium valproate exhibited excitation bands 600 nm and 360nm respectively and sodium valproate emission indicated showed 3 emission bands within near visible region emission observed at (472, 700 and 760nm) and their relative intensities were 2.863, 0.310 and 27.483 respectively. The detection of sodium valproate was accomplished by observing color change of GSH-AgNCs solution from light yellow to brown due to aggregation induced by sodium valproate. GSH-Ag NCs absorbed maximally at 370 nm and after the addition of the drug sodium valproate, the band shifted to 600 nm. The aggregation of GSH-Ag NCs was characterized by UV-Vis spectrometry and fluorimetry, scanning electron microscopy (SEM), energy dispersive X-ray (EDX), Fourier transform infrared spectroscopy (FT-IR), dynamic light scattering (DLS), and zeta potential. Under optimized Conditions, linear calibration curve was obtained within concentration range of 1–8 µg/ml with detection limits of 0.4 µg/ml and limit of quantitation 1.23 µg/ml, respectively. The Fluorescence calibration range was 1–5 µg/ml with limit of detection (LOD) 0.06 µg/ml and limit of quantitation (LOQ) 0.202 µg/ml respectively, showing proposed method to be sensitive. Furthermore, the developed colorimetric assay was found to be simple, sensitive, reproducible and a number of pharmaceutical additives did not affect the determination on a Colorimetric and fluorimetric platform, Sodium valproate was analysed in pharmaceutical formulation, and biological fluids including spiked human urine and blood serum samples with % recoveries of 99.2% and 99.3%.

Keywords: Nanoclusters, sodium valproate, spectrophotometry, spectrofluorometry.

Introduction

Valproic acid (VPA) is an anticonvulsant with broad spectrum of efficiency, but it differs structurally from anti-epileptic medicines.

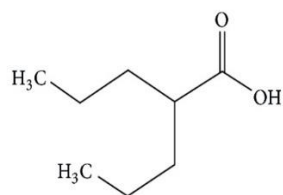


Fig. 1: Structural diagram of Valproic acid

Valproic acid (VPA) is a substance that has been used as an antiepileptic and for stabilizing the mood. The medicine is used for bipolar disorder, epilepsy and less commonly migraine headaches and schizophrenia [1–4]. VPA is considered as a good substitute to phenytoin for the treatment of adult onset epilepsy [5–8]. Side effects are including anorexia, vomiting, and sleep alterations, and are commonly reported in clinical records [9–14]. Sodium valproate is the sodium salt of valproic acid (VPA) with several trade names, including Depalept (sodium valproate) in

the form of an enteric coated tablet for the prolonged release [15, 16]. Sodium valproate is rapidly absorbed after oral administration, reaching peak blood levels within 1 to 4 hours. Chemical structure of valproic acid lacks a chromophore, and hence, it has low absorption, which makes it more difficult to detect to low concentrations. Valproic acid has only weak UV absorbance in the low wavelength range [17, 18]. The determination of valproate acid is reported by gas chromatography (GC) [19], GC-mass spectrometry (GC-MS) [20, 21], high performance liquid chromatography-ultraviolet (HPLC-UV) [22], liquid chromatography-MS/MS (LC-MS/MS) [23, 24], potentiometric biosensor [25], capillary electrophoresis [26] and TLC-densitometric [27] methods. These analytical procedures are highly sensitive, but require expensive equipment with high maintenance cost. The simple procedure involving visual identification and quantitation by simple equipments like spectrophotometer or fluorimeter could be of value. Sorouraddin *et al* [28] reported fluorimetric procedure for the estimation of valproic acid using thioglycolic acid (TGA)-capped CdTe quantum dots.

Nanoclusters (NCs) have attracted the attention as fluorimetric materials for bio imaging [29], catalyst [30] and chemical sensors [31]. These are prepared using different strategies [32, 33]. The applications of silver nanoclusters (AgNCs) are less expensive and indicate adequate sensitivity as sensors [34, 35]. However, AgNCs have somewhat less solution stability in aqueous phase as compared to gold nanoclusters [32]. AgNCs have been used for the determination of a number of analytes including metal ions [7, 35, 37], virus [38], hydrogen peroxide [39], pH [40] and tetracycline [41].

Glutathione (GSH) is naturally occurring tripeptide and is frequently used for the synthesis of gold and silver nanoclusters [42]. GSH not only assists in the preparation, but also stabilise the formed nanoclusters [43, 44]. Sun *et al* [45] synthesised AgNCs by using GSH with σ -lipoid acid and sodium borohydride to form passivated GSH-AgNCs with yellow colour and fluorescence. Slightly modified procedure of Sun *et al* [45] was used for the preparation of GSH-AgNCs for the estimation of sodium valproate with the aid of colorimetric and fluorimetric methods for the detection of sodium valproate from pharmaceutical formulations and biological fluids..

Experimental

Chemicals

All the chemicals used in experimental work were of analytical or Reagent grade. Silver nitrate (AgNO_3), an sodium borohydride (NaBH_4) were from Merck (Darmstadt, Germany. Chemicals Guluthione ($\text{C}_{10}\text{H}_{17}\text{N}_3\text{O}_6\text{S}$). and α -liopic acid (LA) ($\text{C}_8\text{H}_{14}\text{O}_2\text{S}_2$) were obtained from Sigma (Switzerland). Potassium chloride (KCl), Fluka (Switzerland), hydrochloric acid (37%), acetic acid ($\text{C}_2\text{H}_4\text{O}_2$), sodium hydroxide (NaOH), sodium tetraborate decahydrate ($\text{H}_2\text{ONa}_2\text{B}_4\text{O}_{17}$), sodium acetate ($\text{C}_2\text{H}_3\text{NaO}_2$) and boric acid (H_3BO_3) were from Merck (Darmstadt, Germany) and Sigma Aldrich (Switzerland). Sodium valproate standard was kindly provided by Wilshire laboratories (Pvt.) Ltd Karachi, Pakistan. The sodium valproate prescription tablets Epival and capsules were purchased from a nearby pharmacy.

Instrumentation

The UV–Vis absorption spectra of GSH-Ag NCs were recorded on Hitachi 220 double beam spectrophotometer (Hitachi Pvt. Ltd, Tokyo, Japan) employing 1 cm dual quartz cuvettes. Orion 420 A pH meter equipped with glass electrodes and internal

reference electrode (Orion Research In, Boston, USA) was used to confirm pH of buffer solutions. FT-IR Spectra were recorded using Nicolet Atavar 330 (Thermo Nicolet corporation, USA) with attenuated total reflectance accessory (smart partner) within range of $4000\text{--}600\text{ cm}^{-1}$. An Allegra 64 R centrifuge machine (Beckman Coulter, USA) was used to centrifuge sample solutions. The structural and morphological details of GSH-Ag NCs were analyzed on scanning electron microscope (JEOL JSM-6490 LV), at the Centre for Pure and Applied Geology, University of Sindh, Jamshoro. Zeta potential and size distribution of GSH-Ag NCs before and after interaction with sodium valproate were analyzed at Department of Metallurgy and Materials Engineering, Mehran University of Engineering and Technology, Jamshoro by employing Malvern ZS-Nano analyzer (Malvern instrument Inc., London, U.K).

Spectrofluorimetric measurements were made on Shimatzu RF-3501PC (Shimatzu Corporation, Kyoto, Japan) spectrofluorimeter equipped with a xenon discharge lamp and 1 cm quartz cells.

Synthesis of GSH-passivated Ag nanoclusters. Typically, the synthesis of GSH-passivated AgNCs was carried out by slightly modified reported procedure [7, 45]. It was conducted by adding $250\ \mu\text{L}$ AgNO_3 (20 mM) and $300\ \mu\text{L}$ GSH (50 mM) into 10.0 mL ultrapure water at room temperature by magnetic stirring. Then, NaOH (1.0 M) was used to adjust pH to 7.0. At the same time, 10.0 mg LA was mixed with pure sodium borohydride in the molar ratio of LA: $\text{NaBH}_4 = 4:1$ and this was stirred well until a clear solution was observed. Here, LA was first reduced in water to form soluble dihydrolipoic acid (DHLLA). Then, the prepared DHLLA solution was immediately added into the silver mixture by vigorously stirring for one min. Subsequently, a slightly excessive sodium borohydride solution was added drop wise into the mixture. After stirring for 20 min, the mixture was further incubated for 1.5 h at room temperature. The resulting GSH-passivated AgNCs were stored at $4\ ^\circ\text{C}$ in the fridge.

Colorimetric and fluorimetric analysis.

Colorimetric and fluorimetric assays with GSH-passivated AgNCs for sodium valproate were conducted by the following steps. Typically, an aliquot (4.0 mL) of GSH passivated AgNCs were dispersed in the buffer (pH 7.0). Then, a desirable amount of sodium valproate upto ($10\text{--}80\ \mu\text{g}$) and with different concentrations were mixed and further incubated for 5

min. The final volume was adjusted to 10 mL subsequently, the colorimetric and fluorimetric measurements were performed to record the changes of the absorbance and fluorescence intensities of the sensing reactions. The absorbance was measured at 600 nm and fluorescence at 762 nm using excitation at 600 nm.

Analysis of spiked sodium valproate from blood serum

The blood sample (5.0 mL) from healthy volunteer, who had not taken any medication at least for one preceding week, was centrifuged at 6000 g for 20 min. The supernatant layer was collected and added methanol twice in volume. The contents were again centrifuged at 6000 g for 20 min. The deproteinized serum (1.0 mL) from upper layer was transferred to 10 mL volumetric flask and added silver silver nanoclusters solution (4 mL), buffer solution pH 7 (1 mL) and different amounts of sodium valproate were added within calibration range. The final solution was made to the mark. The absorbance and fluorescence of the solutions were measured and quantitation was made from linear regression equations.

Analysis of spiked sodium valproate from urine samples

The urine sample was collected from healthy volunteer and clear urine sample (3.0 mL) was added methanol (6.0 mL) and centrifuged at 6000 g for 20 min. The supernatant layer (1.0 mL) was transferred to volumetric flask (10 mL) and procedure was followed as for blood serum.

The blood and urine samples were collected from healthy volunteers and they were informed the objectives of the study. They gave verbal permission to collect the samples. The blood sample was collected by vein puncture and urine sample was collected in a clean pot. The Ethical committee of Institute of Advanced Research Studies in Chemical Sciences was informed the objectives of the research, and they kindly gave the permission.

Stock solution preparation

The stock solution of standard sodium valproate (1 mg/ml) was prepared by dissolving 25 mg of standard sodium valproate in 25 mL distilled water. The working solution (100 µg/ml) was then prepared by appropriate dilution of stock solution with distilled water.

Preparation of samples for characterization

The sample preparation for characterization by FT-IR and SEM involved centrifugation of sufficient quantity of GSH AgNCs in absence and presence of Sodium valproate at pH 7. The samples were centrifuged at 8000 rpm at room temperature for half an hour. The sample solution containing sodium valproate had the concentration of 10 µg/ml. The supernatant layer was discarded and precipitate (ppts) were collected. The precipitates were added distilled water (15 mL), mixed well and centrifuged at 8000 rpm for 20 min. The upper layer was discarded and precipitates were collected dried at 70 °C. The precipitates in dried powder form were then analyzed by FT-IR, SEM and EDX techniques. The DLS for size distribution and zeta potential of GSH AgNCs without sodium valproate and with sodium valproate were also determined. In this regard, 2 mL of nanoclusters were taken, pH was adjusted to 7 and volume was adjusted to 20 mL. The solution of nanoclusters (2.0 mL) was adjusted to pH 7 and added sodium valproate following the general procedure for detection of sodium valproate. The sample was then diluted up to 20 mL with distilled water. The concentration of sodium valproate in original solution was 10/mL.

Selectivity

4 mL GSH-Ag NCs was transferred into a series of 10 mL volumetric flasks. Then, 1 mL buffer of pH 7, 0.6 mL of 100 µg/mL sodium valproate and 0.6 mL of 1 mg/mL of various interfering species (glucose, sucrose, starch, Na⁺, and Ca²⁺) were added separately. The final volume was adjusted to 10 mL with distilled water. In case of Na⁺ and Ca²⁺, the selectivity was also examined using 1.2 mL of 1 mg/mL of Na⁺ and Ca²⁺ separately. The contents were mixed well and the absorbances were recorded at 600 nm against distilled water. Fluorescences were measured at emission 762 nm and excitation at 600 nm.

Analysis of pharmaceutical preparations

Five tablets of sodium valproate were weighed separately and ground to fine powder. Mass of powder equivalent to 25 mg was dissolved in methanol. The solution was then shaken and filtered to get clear solution. The remaining volume was adjusted with methanol to 25 mL to obtain approximately 1 mg/mL stock solution. The working solution was prepared from stock solution by dilution with methanol. Different concentrations of sodium valproate were taken within calibration range and the solutions were analyzed by following the general

procedure for detection of sodium valproate. Quantitation was then made from linear regression equations using both Spectrophotometric and Fluorimetric procedures.

Results and Discussion

The light yellow solution of glutathione stabilized AgNCs was obtained as a consequence of chemical reduction of AgNO_3 by NaBH_4 in the presence of GSA and LA. In addition, the aggregation of AgNCs was prevented by capping with GSH on the surface of AgNCs [45]. GSA-AgNCs absorbed maximally at 370 nm and fluorimetric study showed maximum with sodium valproate at excitation 600 nm and 660nm respectively and sodium valproate indicated 3 emission bands within near visible region emission observed at (472 , 700 and 762 nm) and their relative intensities were 2.863, 0.310 and 27.483 7 respectively. A systematic study for qualitative and quantitative identification of the drugs using AgNCs as colorimetric and fluorimetric probes were investigated. A number of drugs Artemether, Lumefantrine, Adenocor, Admelog, Pheniramine, Maleate were screened separately by spiking the aqueous solution of AgNCs at optimum pH with the drugs, but these drugs did not indicate any colour reaction. The addition of sodium valproate drug to GSH-AgNCs indicated a prominent colour change of

AgNCs solution from light yellow to brown, may be due to the aggregations of nanoclusters.

Characterization of GSH-Ag NCs Before and after interaction with sodium valproate

The light yellow coloured colloidal solution of GSH-Ag NCs formed was then analyzed by UV–Vis spectrophotometer. Spectral analysis of Ag NCs (Fig.3 a) in absence of Sodium valproate showed a characteristic sharp peak at 370nm. The addition of sodium valproate to GSH-Ag NCs leading to colour change was observed from light yellow to brown with absorbance at 600 nm and a decrease in a surface plasmon resonance band intensity was observed at 370nm (fig3 b).

Characterization of FT-IR, SEM and EDX

The FT-IR spectrum of GSH-Ag NCs without sodium valproate is shown in Fig. 4(a). FT-IR Spectrum of silver nanocluster with Sodium valproate is shown in (Fig 4, b). The SEM image of GSH-Ag NCs without sodium valproate (Fig 4 c) and GSH-Ag NCs with sodium valproate are shown (fig 4 d). The EDX spectrum without drug (fig 4 e) and EDX spectrum with drug are also indicated (fig 4 f).

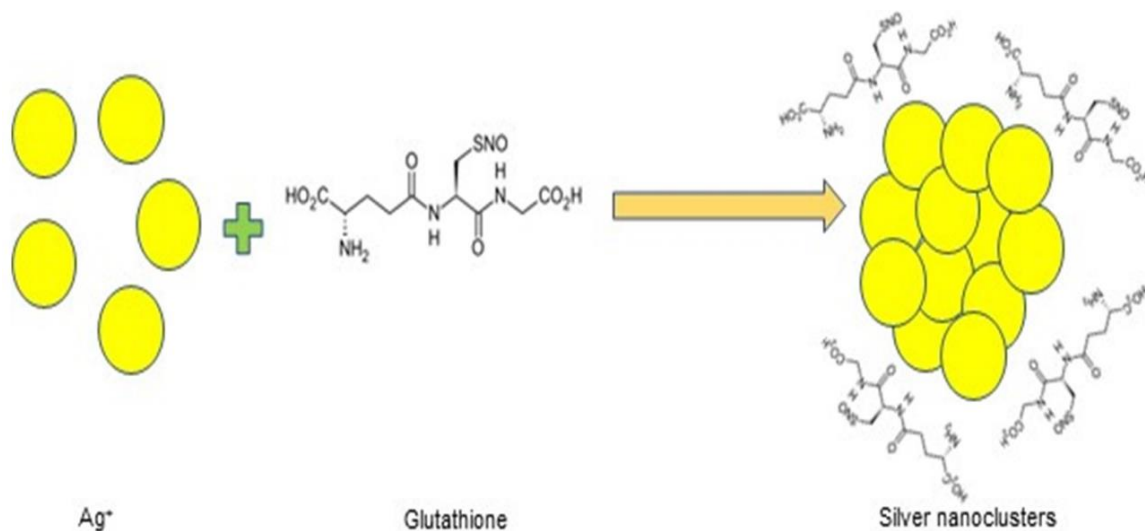


Fig. 2: Schematic representation of glutathione passivated AgNCs.

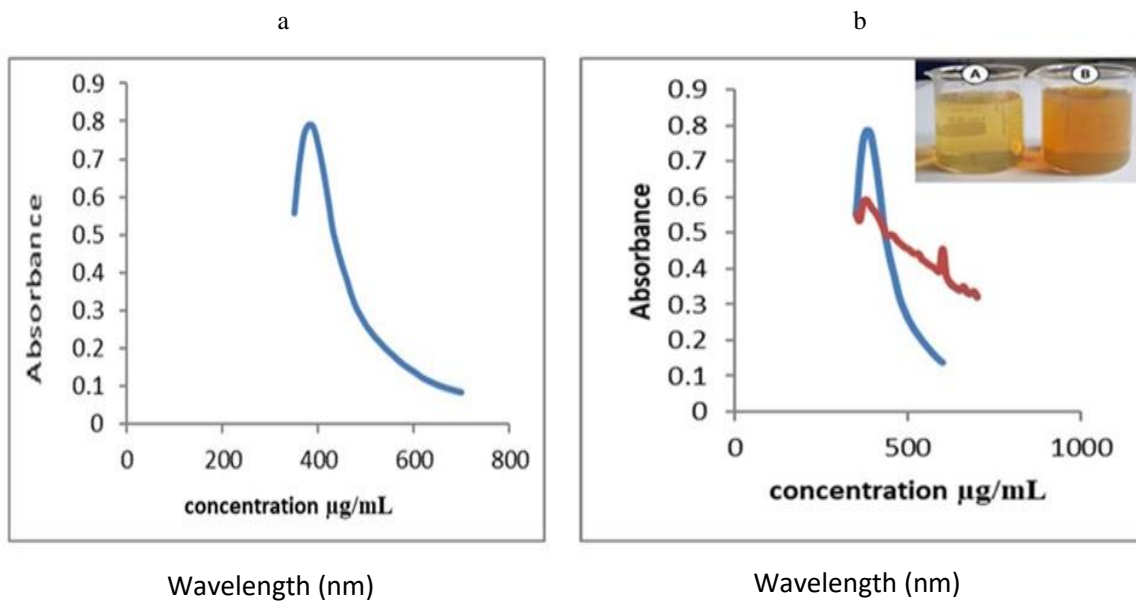


Fig. 3: (a) Visible absorption spectra of GSH-AgNCs in absence of drug and (Fig 3 b) GSH-AgNCs with sodium valproate in presence of drug.

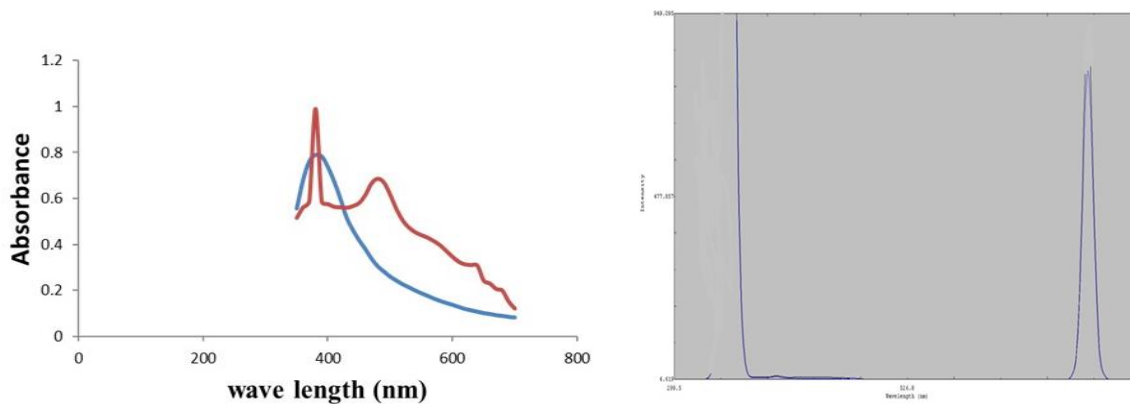
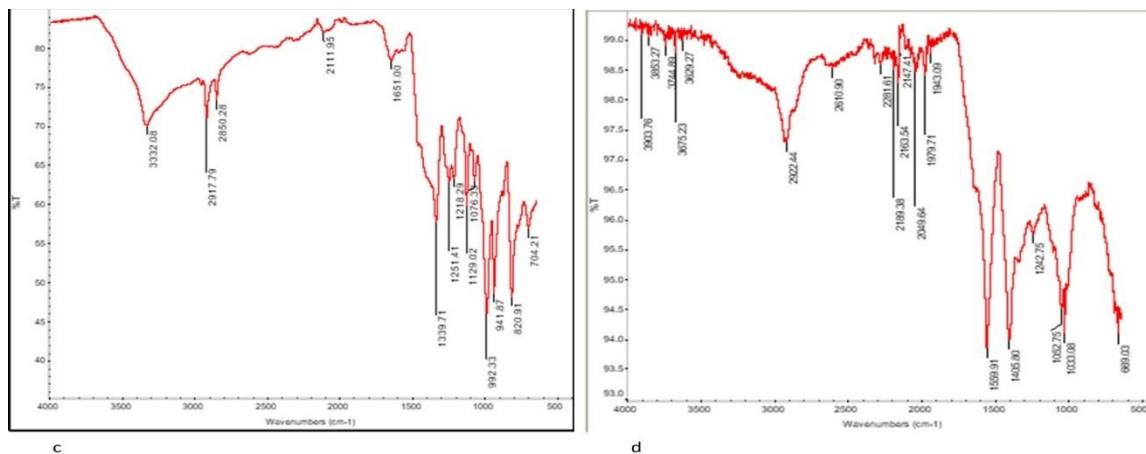


Fig. 3: (c) Spectrofluorometry emission spectra of GSH-AgNCs in absence of drug at wave length 438 nm (fig 3. D) GSH-AgNCs with sodium valproate emission at 762 nm.



c

d

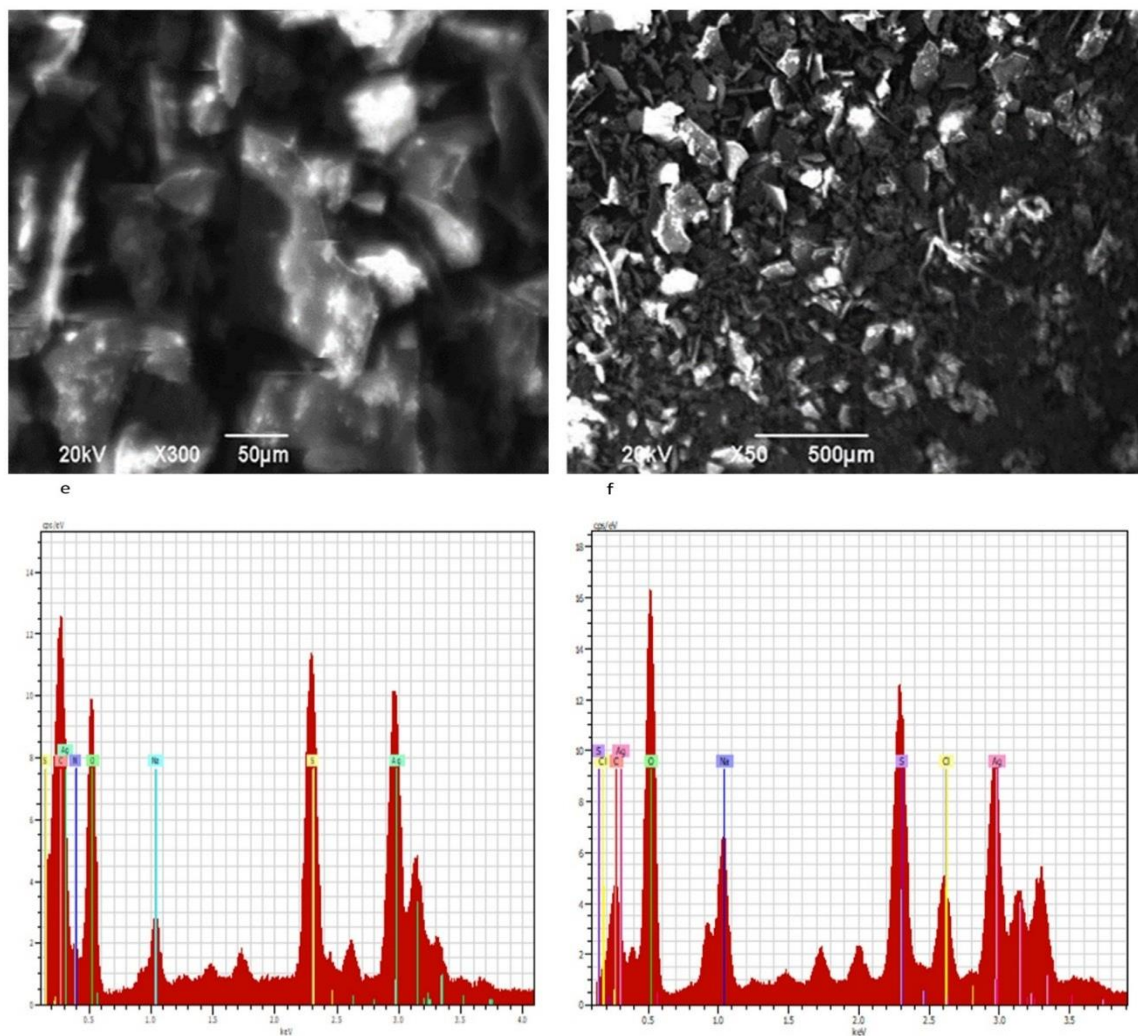


Fig 4: a FT-IR spectra of GSH-AgNCs without sodium valproate and (Fig 4 b) GSH-AgNCs with sodium valproate (10 $\mu\text{g/mL}$) (Fig 4.c) SEM image of GSH-AgNCs without sodium valproate and (Fig 4 d) GSH-AgNCs with sodium valproate (10 $\mu\text{g/mL}$) Fig 4 e EDX GSH-AgNCs without sodium valproate and (Fig 4 f) GSH-AgNCs with sodium valproate (10 $\mu\text{g/mL}$) .

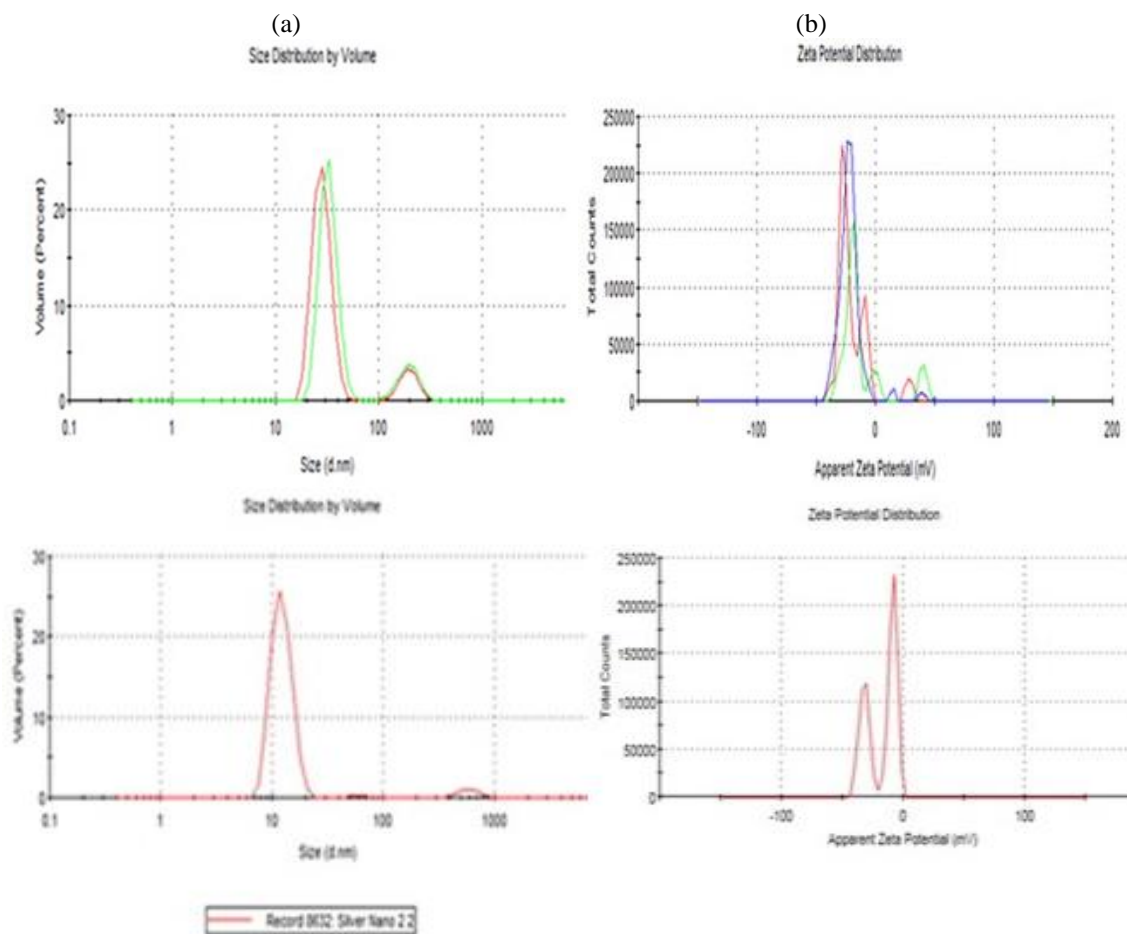
FT-IR for AgNCs indicates peaks corresponding to OH/NH stretching at $3332. \text{cm}^{-1}$, CH at 2917.79 , C=O at $1651. \text{cm}^{-1}$, CH_3 bending at 1339.71 cm^{-1} and 1076.33 cm^{-1} for C=S. Thus, FT-IR suggests the attachment of GSA and LA on the surface of Ag NCs as reported [45]. Although, it can be seen that the intensity of OH/NH stretching vibration of FT-IR spectrum is reduced for GSH-Ag NCs in presence of sodium valproate. Furthermore, it can also be noticed from the FT-IR spectrum of GSH-Ag NCs sodium valproate contains (Fig. 4 b) certain additional peaks confirming the attachment of sodium valproate on the surface of glutathione stabilized Ag NCs thereby inducing aggregation. The peaks for OH/NH 3675.23 cm^{-1} , CH_3 1405.80 cm^{-1} , C-O 1033.08 cm^{-1} , C=O 1559.91 cm^{-1} , 1052 C=S and 669 C-H supports the attachment of sodium valproate to GSH-Ag NCs. Fig

4 c SEM image show that GSH-Ag NCs are of somewhat spherical shape corresponding to dispersed state. However, in presence of sodium valproate, the morphology shows that GSH-Ag NCs is quite different and it seems to be flower-like which confirms the aggregation of Ag NCs (Fig 4 d). EDX of GSH-Ag NCs in the absence and presence of sodium valproate indicated the elements present N, O, Na and S, because sodium valproate contained only the elements C, O and Na which are covered in both (Fig 3 e and f). Another technique which was employed to characterize Ag NCs was dynamic light scattering technique. It involves laser beam to illuminate suspension of particles. From Fig.5 a, it is obvious that the size of Ag NCs is 10 nm in diameter in absence of sodium valproate and the peak is monomodal in nature which further confirms the shape to be spherical [41].

Conversely, three peaks are seen in Fig 5 c in the presence of the drug.. It may be due to flower-like nanoclusters. Moreover, it can also be noticed from Fig 5 a) size distribution of GSH-AgNCs without sodium valproate and Fig 5 b with 100 $\mu\text{g/ml}$ sodium valproate. (Fig. 5) zeta potential of GSH-AgNCs without sodium valproate and (Fig 5 d) with sodium valproate (100 $\mu\text{g/ml}$) that average mean diameter is greatly increased from 10 nm to 198. nm due to interaction of sodium valproate with GSH-Ag NCs. The zeta potential value was total average -17.7 mV for colloidal solution of GSH-AgNCs (Fig.b), indicating the negative charge at surface of Ag NCs. The magnitude of zeta potential value reflects stability of colloidal dispersion due to electrostatic repulsion of negatively charged Ag NCs which is consistent with reported procedures [42, 43] From (Fig. 5 d) it is clear that total average of zeta potential value is -2. mV due to interaction of positively charged sodium valproate with negatively charged GSH-Ag NCs. It results in an increase in electrostatic forces among nanoparticles leading to aggregation thereby decreasing the stability of Ag NCs.

Effect of pH

The effect of pH on absorbance of GSH-Ag NCs in presence of sodium valproate was investigated from pH 2–10 by monitoring concentration within the UV–Vis and florescence within the wavelength range of 360–765 nm. As, it is clear from Fig. 5 a,b that the maximum absorbance occurred at pH 7 and was selected. Moreover, it was observed during study of pH effect that at lower pH (< 4), the GSH-Ag NCs solution was unstable and the aggregation occurred without adding any analyte, resulting in color change of Ag NCs solution from light yellow to colorless which is in accordance with reported literature [44]. This was due to neutralization of surface charge of Ag NCs. However, at higher pH values i.e. > 7 and < 11 , the GSH-AgNCs were stable, the characteristic color of Ag NCs solution remained bright yellow even after addition of buffer solution. The addition of sodium valproate to GSH-Ag NCs at pH 7 lead to color change from yellow to brown due to aggregation induced by sodium valproate.



Factors influencing colorimetric and fluorimetric sensing

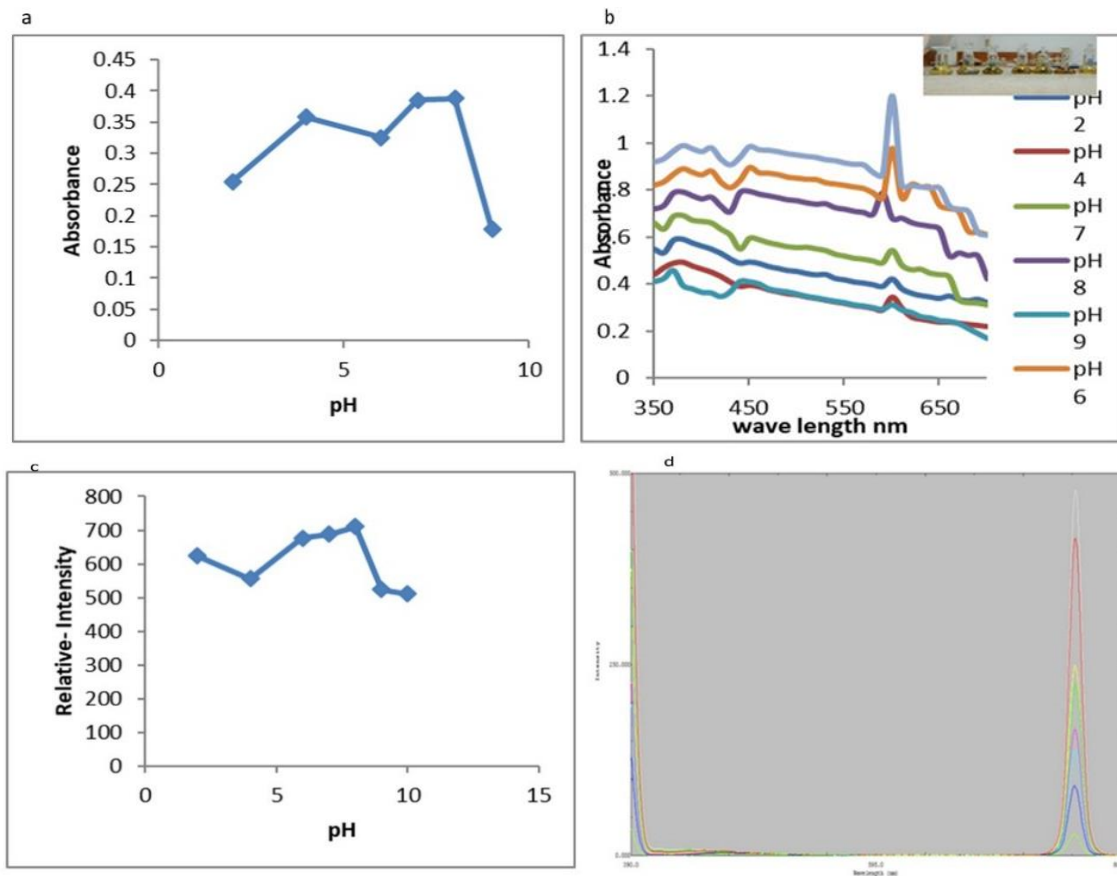


Fig. 6: a , b) and (Fig 6 c , d) Uv-Vis absorption spectra and spectrofluometry image of GSH-AgNCs with sodium valproate with 100 $\mu\text{g/ml}$ pH 2-10.

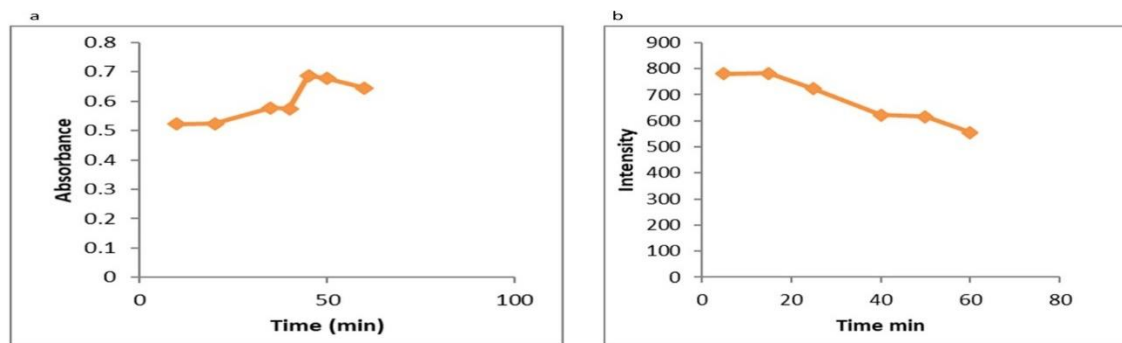


Fig. 7: a effect of time on spectrophotometer and (Fig 7 b) effect of time on spectrofluorimetry.

Effect of time

The influence of time on absorbance and fluorescence of GSH-Ag NCs was studied for 1h in presence of 10 $\mu\text{g/ml}$ sodium valproate at pH 7 as shown in Fig. 7 a, b.. The absorbance of the sample solution was recorded within 5 min at 600 nm then at

an interval of 15 min. The fluorescence emission was measured at 760nm. It was found that absorbance after 5 min remained nearly constant up to 50min. Thus, 45 min was chosen as an optimum time for study of absorption after addition of sodium valproate.

Effect of concentration of sodium valproate

To investigate the influence of concentration of sodium valproate on absorbance, the calibration curve was plotted within concentration range of 1-8 $\mu\text{g/ml}$. The Fluorescences was within concentration range 1-5 $\mu\text{g/ml}$. Fig 7 b, d shows that the relative intensity is increased with sodium valproate R^2 0.9876. Fig 8 a shows that the absorption ratio at A600/A370 is increased with increase in sodium valproate concentration with R^2 0.9956. Moreover, it was also observed that color of GSH-Ag NCs solution changed

from light yellow to brownish yellow and then to brown upon increasing sodium valproate concentration. This enables one to determine sodium valproate by naked eye. The limit of detection (LOD) and limit of quantitation (LOQ) were calculated from 3.3 and 10.0 times the standard deviation of slope divided by the slope of calibration curve using linear regression equation and were found to be 0.40 and 1.23 $\mu\text{g/ml}$, respectively, The limit of detection (LOD) and limit of quantitation (LOQ) were found 0.06 $\mu\text{g/ml}$ and 0.202 $\mu\text{g/ml}$ respectively, showing proposed method to be sensitive.

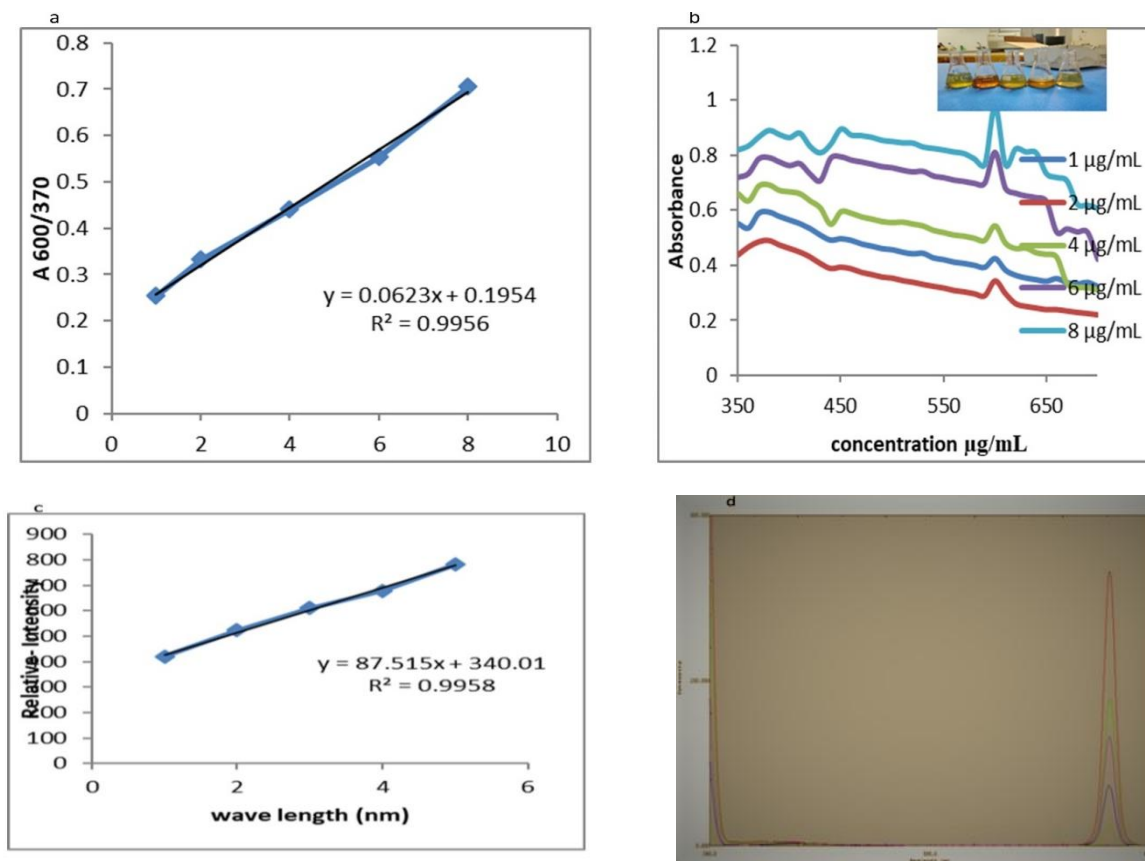


Fig. 8: (a, b) Calibration graph of absorption ratio of GSH-AgNCs various concentration with sodium valproate 1-8 $\mu\text{g/ml}$ and (Fig c, d) in spectrofluorimetry various concentration with 1-5 $\mu\text{g/ml}$.

Intra-day and inter-day variation

Intra-day and inter-day precision were evaluated at a concentration of sodium valproate 6 $\mu\text{g/ml}$ under optimum conditions. The relative standard deviation (RSD) was found to be $< 2.8\%$ ($n = 5$) for both intra-day and inter-day precision assays. This shows that our developed method is highly repeatable and reproducible.

Table-1a: Intra-day and Inter-day variation on spectrophotometer of sodium valproate

| Concentration of standard ($\mu\text{g/ml}$) | Intra day | Inter day |
|--|-----------|-----------|
| % RSD (n=5) | 1.66 | 2.8 |

Table-2b: Intra-day and Inter-day variation on fluorescences of sodium valproate.

| Concentration of standard ($\mu\text{g/ml}$) | Intra day | Inter day |
|--|-----------|-----------|
| % RSD (n=5) | 1.8 | 2.2 |

Selectivity of method

The selectivity of the proposed colorimetric assay was examined by adding various pharmaceutical additives including glucose, sucrose, starch, Ca²⁺, and Na⁺ to GSH Ag NCs solution individually in a concentration 10 times more than the concentration of sodium valproate under optimum conditions. The concentration of sodium valproate was 6 µg/ml, and for Fluorescence concentration was 4 µg/ml. A relative error of below 3% was obtained (Fig.9 a b). It was found that absorbance remained almost similar even in presence of foreign species. In case of Na⁺ and Ca²⁺, the selectivity was also investigated at a concentration of 80µg/ml. The results indicate that Na⁺ did not interfere at higher

concentration and the relative error was -2.5%. However, Ca²⁺ indicated relative error -5.5%. It shows that Ca²⁺ is not interfering at this concentration.

Analysis of sodium valproate in pharmaceutical formulation and biological fluids

Sodium valproate was determined in commercially available Epival tablet containing 20 mg sodium valproate. The RSD calculated was < 2% (n = 3) with the recoveries ranged from 99 to 99.07%. The amount found agreed well with the labelled amount on packet .Fig 10,a

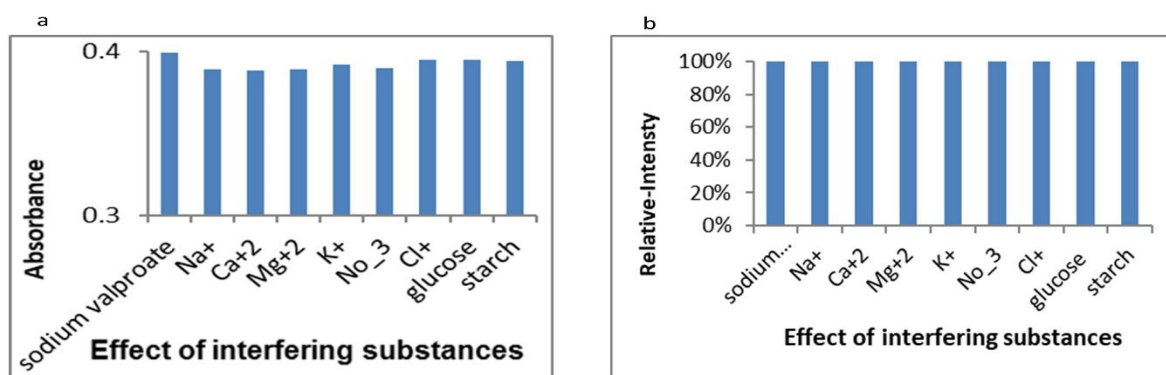


Fig. 9: a) UV-Vis absorption spectra and fluorescences of Interference effect of pharmaceutical additives (sodium valproate 6 µg/ml, additives 60 µg/ml) (Fig 9 b) Fluorescences sodium valproate 4 µg/ml additives 40 µg/ml.

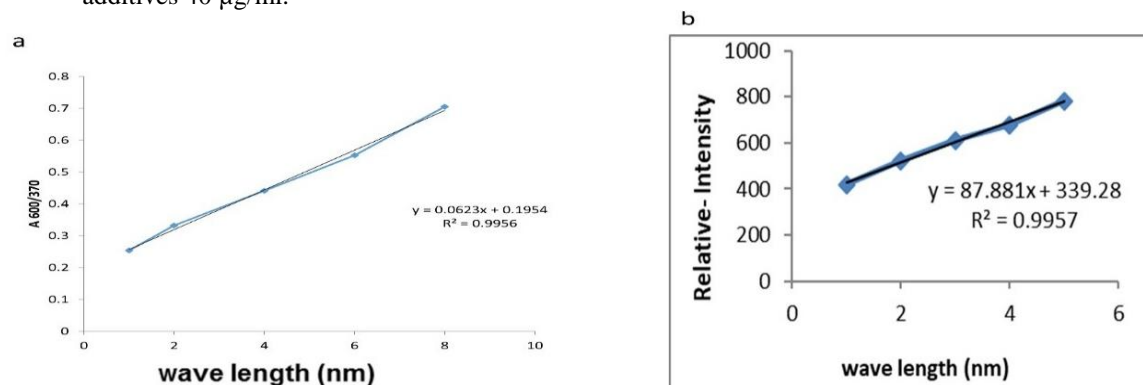


Fig. 10: a) Spectrophotometer calibration graph of absorption ratios of silver nanocluster with sodium valproate in blood serum. (Fig 10 b) fluorescences calibration graph of silver nanocluster with sodium valproate in blood serum.

Table-2: a) Analysis of Sodium valproate pharmaceutical preparations.

| Drug | Analyte Standard | Added amount (milligram/tablet) | Found amount (milligram/tablet) | Recovery % | % Error |
|--------|------------------|---------------------------------|---------------------------------|------------|---------|
| Epival | Sodium valproate | 20.0 | 19.2 | 99.39 | ±4.5 |
| | | 20.0 | 19.4 | 99.09 | ±2.4 |
| | | 20.0 | 19.4 | 99.09 | ±3.8 |
| Epival | Sodium valproate | 20.0 | 19.2 | 99.56 | ±2.4 |
| | | 20.0 | 19.7 | 99.98 | ±3.4 |
| | | 20.0 | 19.2 | 99.45 | ±2.16 |
| | | 20.0 | 19.2 | 99.45 | ±2.16 |

Analysis of sodium valproate by standard addition method

Sodium valproate was also analysed by standard addition technique. Different amounts of standard of Sodium valproate were added to the drug solution of sodium valproate. The concentration of drug solution was constant i.e 4 µg/ml while the standard was added in a concentration of 2, 4, 6 µg/ml separately in each sample of drug solution except the first one which remained un added. The samples were examined on spectrophotometer against distilled water. The absorbance of each of the sample solution was measured at 600 nm and the increase in absorbance was found with increase in amount of the added standard. The fluorescences analysed by standard addition of different amount of sodium valproate 2 µg/ml, while the standard was added in a concentration of 1,2,4 µg/ml respectively. The absorbance of the sample solution was measured at 600nm and emission at 762 nm. The total amount of the drug found containing Sodium valproate in its pure form along with sodium valproate in dosage form was calculated from linear regression equation of standard sodium valproate. Furthermore, the sodium valproate was also analyzed by standard addition method. The results are summarized in Table-3. Similarly, the developed colorimetric and fluorimetric assay was applied to analyze sodium valproate in biological fluids including spiked human urine and blood serum samples. RSDs for spiked human urine and blood serum samples were $\pm 5.0\%$ and $\pm 2.8\%$ (n = 3), respectively, with recoveries of 99.39–99.09%. Additionally, the urine sample was also analyzed after deproteinization. The spiked sample indicated

recovery of 99.56-99.45%. This supports that human urine and blood serum samples did not interfere the determination of sodium valproate.

The results of sensitivity and easy of analysis were compared to those of other published methods (Table-5).

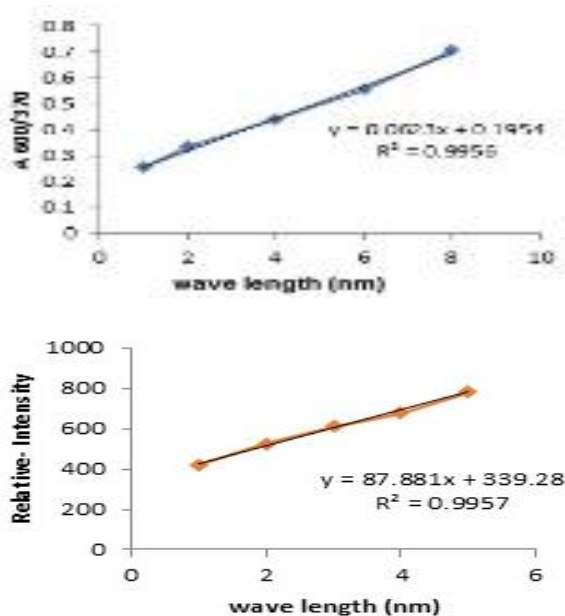


Fig. 11: a) spectrophotometer calibration graph of absorption ratios of silver nanoclusters with sodium valproate spiked urine serum (Fig11 b) fluorescences calibration graph of silver nanoclusters with sodium valproate urine serum.

Table-3: a) Analysis of blood serum and urine serum in sodium valproate.

| Sample | Analyte standard | Added amount (µg/ml) | Found amount (µg/ml) | Recovery % | % Error |
|-------------|------------------|----------------------|----------------------|------------|-----------|
| Blood serum | Sodium valproate | 2 | 2.100 | 99. | ± 5.0 |
| | | 6 | 6.126 | 99.09 | ± 2.8 |
| | | 4 | 4.421 | | ± 4.7 |
| Urine serum | Sodium valproate | 2 | 2.111 | 99.56 | ± 5.0 |
| | | 6 | 6.217 | 99.57 | ± 3.4 |
| | | 4 | 4.251 | 99.45 | ± 5.9 |

Table-4: a) Comparison of previous published work with present work.

| Analyte | Analytical technique | Calibration range (µM) | LOD (µM) | Sample analyzed | References |
|------------------|---|------------------------|---------------|--|------------|
| Sodium valproate | Spectrophotometric | 24-114 | 0.24 | Urine sample | [1] |
| | Ultraperformance Liquid Chromatography | 2-20 and 1-8µg/mL | 0.2 -0.5µg/mL | Pharmaceuticals and plasma | [4] |
| | UPLC | 50-400 | | | |
| Sodium valproate | Gas Chromatography | 50-150µg/m-1 | 1.0-10 | Pharmaceutical formulations | [20] |
| | | | | Urine | |
| Sodium valproate | | | 0.083 | Pharmaceutical preparations | [25] |
| | | | | Tablets | |
| Sodium valproate | AgNCs based colorimetric sensor and Fluorimetric sensor | 1-8 1-5µg/mL | 0.2-0.4µg/mL | pharmaceuticals, spiked human urine, and blood serum | This work |

Conclusions

A new colorimetric and fluorimetric sensing approach was developed for the analysis of sodium valproate in pure form, pharmaceutical preparation, spiked human urine and blood serum samples using GSH-Ag NCs. The experimental parameters were studied and the best pH for colorimetric and fluorimetric sensing of sodium valproate was found to be 7. The proposed techniques are simple, reliable, sensitive and selective. LOD and LOQ were found to be 0.2 and 0.6 µg/ml, respectively. The colorimetric and fluorimetric platform made it possible to detect sodium valproate visually on the basis of color change of Ag NCs from light yellow to brown within few minutes without requiring any special additives and expensive instrumentation. This simple and speedy analytical approach would hold great potential for detection of sodium valproate in clinical analysis.

Acknowledgement

We gratefully acknowledge University of Sindh, Jamshoro, Pakistan for supporting the research project financially. We like to thank Wilshire Laboratories (Pvt) Ltd, Karachi, Pakistan for very kindly providing the standard of sodium valproate. We also like to thank Professor Dr Abdullah Dayo, Dean Faculty of Pharmacy, University of Sindh for his help in getting the standard of sodium valproate.

References

1. T. R. Henry, The history of valproate in clinical neuroscience, *Psychopharmacol. Bull*, **37**, 5, (2003).
2. G. Rosenberg, The mechanisms of action of valproate in neuropsychiatric disorders: can we see the forest for the trees?," *CMLS*, **64**, 2090 (2013).
3. E. Posner and N. Lorenzo, Posttraumatic epilepsy in children and adults and valproates, *Mizhnarodnyi Nevrolohichnyi Zhurnal*, **1**, 43, (2006).
4. MediLexicon International Ltd, FDA Issues Approvable Letter for Stavzor Delayed Release Valproic Acid Capsules, (2007).
5. R. Seymour, D. Smith, and D. Turnbull, The effects of phenytoin and sodium valproate on the periodontal health of adult epileptic patients," *J. Clin. Periodontol*, **12**, 413 (1985).
6. B. Dannewitz, E. M. Kruck, H. J. Staehle, P. Eickholz, T. Giese, S. Meuer, V. Kaefer, M. Zeier, and C. Sommerer, Cyclosporine-induced gingival overgrowth correlates with NFAT-regulated gene expression: a pilot study, *J. Clin. Periodontol*, **38**, 984 (2011).
7. B. Adhikari and A. Banerjee, Facile synthesis of water-soluble fluorescent silver nanoclusters and HgII sensing, *Chem. Mater.* **22**, 4364 (2010).
8. O. Nakade, D. J. Baylink, and K. H. W. Lau, Osteogenic actions of phenytoin in human bone cells are mediated in part by TGF-β1, *JBMR®*, **11**, 1880 (1996).
9. T. Percival, S. Aylett, F. Pool, A. Bloch-Zupan, G. Roberts, and V. Lucas, Oral health of children with intractable epilepsy attending the UK National Centre for Young People with Epilepsy, **10**, 19 (2009).
10. J. L. Herranz, R. Arteaga, and J. A. Armijo, Side effects of sodium valproate in monotherapy controlled by plasma levels: a study in 88 pediatric patients, *Epilepsia*, **23**, 2 (1982).
11. J. M. Avari, Paradoxical agitation in adolescent male on valproate, *J. Child Adolesc. Psychopharmacol.* **26**, 78 (2016).
12. N. Taşer and M. Sarıkaya, An unusual case of pleuropericardial neutrophilic effusion associated with valproate *JFMA*, **114**, 375 (2013).
13. W. R. Yamak, G. Hmameess, Y. Makke, S. Sabbagh, M. Arabi, A. Beydoun, and W. Nasreddine, Valproate-induced enuresis: a prospective study, *DMCN*, **57**, 737 (2015).
14. G. D. Anderson, Y. X. Lin, C. Berge, and G. A. Ojemann, Absence of bleeding complications in patients undergoing cortical surgery while receiving valproate treatment, *J. Neurosurg*, **87**, 252 (1997).
15. M. E. Ivan, M. M. Safaee, N. L. Martirosyan, A. Rodríguez-Hernández, B. Sullinger, P. Kuruppu, J. Habdank-Kolaczkowski, and M. T. Lawton, Anatomical triangles defining routes to anterior communicating artery aneurysms: the junctional and precommunicating triangles and the role of dome projection, *J. Neurosurg*, **132**, 1517 (2019).
16. E. Kingsley, P. Gray, k. G. Tolman, and R. Tweedale, The toxicity of metabolites of sodium valproate in cultured hepatocytes, *J. Clin. Pharmacol.* **23**, 178 (1983).
17. R. Gugler and G. E. von Unruh, Clinical pharmacokinetics of valproic acid, *Clin. Pharmacokinet*, **5**, 67 (1980).
18. A. A. Matin, P. Biparva, H. Amanzadeh, and K. Farhadi, Zinc/Aluminum layered double hydroxide-titanium dioxide composite nanosheet film as novel solid phase microextraction fiber for the gas chromatographic determination of valproic acid, *Talanta*, **103**, 207 (2013).
19. L. Rhodes, M. Benzine, P. Hidalgo, C. A. da Silva, R. Linden, Simple procedure for determination of valproic acid in dried blood

- spots by gas chromatography-mass spectrometry, *JPBA*, **97**, 207 (2014).
20. V. D. Schaefer, L. de Lima FeltracoLizot, R. Z. Hahn, A. Schneider, M. V. Antunes, R. Linden, Simple determination of valproic acid serum concentrations using BioSPME followed by gas chromatography-mass spectrometric analysis, *J. Chromatogr. B Biomed. Appl.* **1167**, 122574 (2021).
 21. Z.-J. Chen, X.-d. Wang, H.-s. Wang, L.-m. Zhou, J.-l. Li, W.-y. Shu, J.-q. Zhou, Z.-y. Fang, Y. Zhang, and M. Huang, Simultaneous determination of valproic acid and 2-propyl-4-pentenoic acid for the prediction of clinical adverse effects in Chinese patients with epilepsy, *Seizure*, **21**, 110 (2012).
 22. S. Gao, H. Miao, X. Tao, B. Jiang, Y. Xiao, F. Cai, Y. Yun, J. Li, and W. Chen, LC-MS/MS method for simultaneous determination of valproic acid and major metabolites in human plasma, *J. Chromatogr. B Biomed. Appl.* **879**, 1939 (2011).
 23. O. Özbek, Ö. Isildak, and I. Isildak, A potentiometric biosensor for the determination of valproic acid: human blood-based study of an anti-epileptic drug, *Biochem. Eng. J.* **176**, 108181 (2021).
 24. G. K. Belin, S. Krähenbühl, and P. C. Hauser, Direct determination of valproic acid in biological fluids by capillary electrophoresis with contactless conductivity detection, *J. Chromatogr. B Biomed. Appl.* **847**, 205 (2007).
 25. W. Parts, A. Pyka-Panama, Use of TLC-densitometric method for determination of valproic acid in capsules, *Molecules*, **27**, 752, (2022).
 26. M. H. Sorouraddin, A. Imani-Nabiyi, S. A. Namibian-Gehraz, M. R. Rashidi, A new fluorimetric method for determination of valproic acid using TGA-capped CdTe quantum dots as proton sensor, *J. Lumin.* **145**, 253 (2014).
 27. B. Z. Chi, C. L. Wang, Z. Q. Wang, T. Pi, X.-L. Zhong, C.-Q. Deng, Y. C. Feng, Z. M. Li, Fluorometric determination of the bio marker terminal deoxynucleotidyl transferase via the enhancement of the fluorescence of silver nanoclusters by in-Situ grown DNA tails, *Mikrochim. Acta* **186**, 241 (2019).
 28. Y. Du, H. Sheng, D. Astruc, M. Zhu, Atomically precise Nobel metal nanoclusters as efficient catalyst: a bridge between structure and properties, *Chemical Reviews*, **120**, 526 (2020).
 29. K. Saha, S. S. Agassi, C. Kim, X. Li, V. M. Rolello, Gold nanoparticles in chemical and biological sensing, *Chem. Rev.* **112**, 2739 (2012).
 30. Y. P. Xie, Y. L. Shen, G. X. Duan, J. Han, L. P. Zhang, X. Ku, Silver nanoclusters: synthesis, structure and photo luminescence, *Mater. Chem. Front*, **4**, 2205 (2020).
 31. H. Xu, K. S. Suslick, Water-soluble fluorescent silver nanoclusters, *Adv. Mater.* **22**, 1078 (2010).
 32. K. Chaiendoo, S. Samarinda, S. Kulchat, V. Promarak, T. Tuntulani, W. Ngeontae, A new formaldehyde sensor from silver nanoclusters modified Tollens reagent, *Food Chemistry*, **255**, 41 (2018).
 33. N. Cao, J. Xu, H. Zhou, Y. Zhao, J. Xu, J. Li, and S. Zhang, A fluorescent sensor array based on silver nanoclusters for identifying heavy metal ions, *Microchem. J.*, **159**, 105406 (2020).
 34. B. Adhikari and A. Banerjee, Facile synthesis of water-soluble fluorescent silver nanoclusters and HgII sensing, *Chem. Mater.* **22**, 4364 (2010).
 35. L. Shang and S. Dong, Silver nanocluster-based fluorescent sensors for sensitive detection of Cu (II), *Chem. Mater.* **18**, 4636 (2008).
 36. D. Li, H. Chen, X. Gao, X. Mei, L. Yang, Development of general methods for detection of virus by engineering fluorescent silver nanoclusters, *ACS Sensors*, **6**, 613 (2021).
 37. A. S. Patel and T. Mohanty, Silver nanoclusters in BSA template: a selective sensor for hydrogen peroxide, *J. Mater. Sci.* **49**, 2136 (2014).
 38. F. Qu, N. B. Li, and H. Q. Luo, Highly sensitive fluorescent and colorimetric pH sensor based on polyethylenimine-capped silver nanoclusters, *Langmuir*, **29**, 1199 (2013).
 39. C. Liu, Y. Ding, Q. Li, and Y. Lin, Photochemical synthesis of glutathione-stabilized silver nanoclusters for fluorometric determination of hydrogen peroxide, *Mikrochim. Acta*, **184**, 2497 (2017).
 40. N. Cao, H. Zhou, H. Tan, R. Qi, J. Chen, S. Zhang, and J. Xu, Turn-on fluorescence detection of cysteine with glutathione protected silver nanoclusters, *MAF*, **7**, 034004 (2019).
 41. F. Qu, N. B. Li, H. Q. Luo, Highly sensitive fluorescent and colorimetric pH sensor based on polyethylenimine-capped silver nanoclusters, *Langmuir*, **29**, 1199 (2013).